

## **General Disclaimer**

### **One or more of the Following Statements may affect this Document**

- This document has been reproduced from the best copy furnished by the organizational source. It is being released in the interest of making available as much information as possible.
- This document may contain data, which exceeds the sheet parameters. It was furnished in this condition by the organizational source and is the best copy available.
- This document may contain tone-on-tone or color graphs, charts and/or pictures, which have been reproduced in black and white.
- This document is paginated as submitted by the original source.
- Portions of this document are not fully legible due to the historical nature of some of the material. However, it is the best reproduction available from the original submission.

NASA Technical Memorandum 82968

(NASA-TM-82968) FUNDAMENTAL ASPECTS OF  
POLYIMIDE DRY FILM AND COMPOSITE  
LUBRICATION: A REVIEW (NASA) 42 p  
HC A03/MF A01

N83-14271

CSCL 11H

Unclas

G3/27 02293

# Fundamental Aspects of Polyimide Dry Film and Composite Lubrication—A Review

Robert L. Fusaro  
*Lewis Research Center*  
*Cleveland, Ohio*



Prepared for the  
Joint Lubrication Conference  
cosponsored by the American Society of Mechanical Engineers  
and the American Society of Lubrication Engineers  
Washington, D.C., October 5-7, 1982

**NASA**

# FUNDAMENTAL ASPECTS OF POLYIMIDE DRY FILM AND COMPOSITE LUBRICATION - A REVIEW

Robert L. Fusaro

National Aeronautics and Space Administration

Lewis Research Center

Cleveland, Ohio 44135

## ABSTRACT

This paper reviews the research conducted to date at NASA Lewis Research Center on the fundamental tribological properties of polyimide dry films and composites. Friction coefficients, wear rates, transfer film characteristics, wear surface morphology, and possible wear mechanisms of several different polyimide films, polyimide-bonded solid lubricants, polyimide solid bodies, and polyimide composites are compared and discussed. Such parameters as temperature, type of atmosphere, load, contact stress, and specimen configuration are investigated. In addition, data from an accelerated test device (Pin-on-Disk) are compared to similar data obtained from an end-use application test device (plain spherical bearing).

## INTRODUCTION

There are continually increasing needs in the aerospace industry for self-lubricating materials which will function at higher and higher temperatures. Self-lubricating materials are needed for air bearings, journal bearings, spherical bearings, ball bearings, gears, seals, etc. (1 to 7).

Polyimide is one class of thermally stable organic polymers which has demonstrated considerable potential for these applications. Polyimide refers to a general class of long-chain polymers which have repeated imide groups as an integral part of the main chain. Polyimides of different chemical composition and structure can be obtained by varying the monomeric constituents. In general, the polyimide chains consist of aromatic rings alter-

nated with heterocyclic groups. Because of the multiple bonds between these groups, the polyimides are characterized by a relatively high thermal stability (400° C in air, 500° C in inert atmospheres) (8 to 10). Their radiation stability is also high, being able to withstand high exposure to neutrons, electrons, ultraviolet light, and gamma radiation (8, 11, and 12). They resist most common chemicals and solvents, but are attacked by alkaline materials (11 and 12). At the decomposition point, they crumble to a fine powder without melting. For a more detailed discussion of the physical properties, see (8 to 13).

It has been demonstrated in previous studies (9 and 10, 14 to 17) that polyimide films or polyimide-bonded graphite fluoride films have considerable potential for self-lubrication applications such as foil bearings, where long thermal soaks are encountered. Low weight loss rates, good adhesion, and good friction and wear characteristics were obtained for temperatures to 315° C in air (10 and 14).

Solid bodies of polyimide can also be employed in dry bearings, seals, gears, etc. In many applications, polyimide by itself is sufficient to improve the tribological properties of the intended end-use part. However, in many instances, solid lubricant additives are needed to improve lubrication. Powdered solid lubricants added to polyimide solids or films can improve the friction and wear characteristics, but they also can reduce the load-carrying capacity. To improve the load-carrying capacity of polyimide solid bodies, reinforcing fibers can be incorporated. If graphite fibers are used, in addition to improving the strength and stiffness of the polyimide, improved lubrication performance can be obtained. Considerable research has gone into developing graphite fiber reinforced polyimide (GFRPI) composite materials (1, 4, 5, 7, and 18 to 34).

Research has also been conducted at the NASA Lewis Research Center on the fundamental aspects of polyimide dry film and composite solid body lubrication. The purpose of this paper is to review and summarize that work.

## MATERIALS

Nine different types of polyimides were compared in this study. Those with known compositions are given in Fig. 1. Seven of the polyimides were evaluated as films, and were designated PIC - 1 to PIC - 7. Three of the polyimides were made into solid bodies or composites and were designated types "A," "C," or "V". The polyimide film PIC - 7 and the polyimide solid type "C" are the same polyimide. Polyimide type "V" is used to formulate commercially available composites.

The polyimide films (20 to 25 $\mu$ m thick) were applied to sandblasted AISI 440C HT (high temperature) stainless steel disk substrates (Rockwell hardness, C-60; surface roughness, 0.9 to 1.2  $\mu$ m (cla)). Polyimide-bonded films were made using type PIC-1 polyimide and 75 wt percent molybdenum disulfide ( $\text{MoS}_2$ ) or 50 wt percent graphite fluoride ( $(\text{CF}_{1.1})_n$ ). One commercially available composite made with type "V" polyimide and 15 percent graphite powder was evaluated. Three different composites were made using type "A" and type "C" polyimides and 50 wt percent of chopped graphite fibers. Two types of chopped fibers were used, a low modulus fiber (type "L") and a high modulus fiber (type "H"). Fiber properties are given in Table 1. For more details on the films or composites see Refs. (23 and 26).

Hemispherically tipped pins of radius 0.475 cm were made of AISI 440C HT stainless steel (Rockwell hardness, C-60; surface roughness, cla 0.1 $\mu$ m) of the composite material. The 440C HT pins were slid against the films or the composite disks and the composite pins were slid against 440C HT disks with surface roughnesses less than 0.1  $\mu$ m, cla.

## EXPERIMENTAL PROCEDURE

A pin-on-disk tribometer was used in this study (Fig. 2). The riders were either hemispherically tipped pins with a radius of 0.475 cm or the same hemispherically tipped pins with 0.67, 0.95, 1.35, or 1.75 mm diameter flats worn on them (see insert Fig. 2). They were loaded with a 9.8 N dead weight against the disk which was rotated at 1000 rpm. The pin slid on the disk at a radius of 2.5 cm giving it a linear sliding speed of 2.7 m/s. The test specimens were enclosed in a chamber so that the atmosphere could be controlled. Atmospheres of dry argon (<100 ppm H<sub>2</sub>O), dry air (<100 ppm H<sub>2</sub>O), or moist air (10 000 ppm H<sub>2</sub>O) were evaluated.

Each test was stopped after predetermined intervals of sliding and the pin and disk were removed from the friction apparatus. The contact areas were examined by optical microscopy and photographed, and surface profiles of the disk wear track were taken. Locating pins insured that the specimens were returned to their original positions. Disk wear was determined by measuring the cross-sectional area on the disk wear track (from surface profiles), and rider wear was determined by measuring the wear scar diameter on the hemispherically tipped rider after each sliding interval and then calculating the volume of material worn away.

## RESULTS AND DISCUSSION

### Polyimide - Solid Bodies and Films

Wear Mechanisms -- 25° C - The wear process of a polyimide solid body or composite body is one of gradual wear through the body. A film, however, can lubricate by either of two processes. It can support the load and be worn away gradually, similar to a solid body; or it can be quickly worn away with the subsequent formation of a secondary film at the substrate interface. In the second instance, shearing of the secondary film provides the lubri-

cation. Figure 3 gives cross-sectional areas of a film wear track illustrating these two mechanisms. When the lubrication process is one of gradual wear through the body or film, generally no measurable wear occurs to the metallic pin. But when the lubrication process is of the secondary film type, wear of the rider increases (usually at a constant rate) with sliding distance, probably because some metal-to-metal contact occurs during the shearing of the film.

The seven polyimide films evaluated were all able to lubricate by either mechanism, although the gradual wear through the film mechanism is preferred since minimal wear to the metallic pin occurs. However, for this mechanism it was found that the different polyimides produced different friction coefficients and different wear rates.

Friction and Wear - 25° C - The general trend for the wear of the polyimide films or solid bodies was to increase in a linear manner (from zero) as a function of sliding distance. Figure 4 plots wear volume for representative polyimides as a function of sliding distance. Wear rates were determined by taking a linear regression fit (least squares) of these data. Average wear rates are given for each polyimide evaluated in Table 2.

The table also gives the average "steady-state" friction coefficient obtained for each polyimide. The table indicates that the three films that gave the lowest friction coefficients also gave the highest wear rates. The four other films and the type "V" polyimide solid body gave higher friction coefficients but lower wear rates. The polyimide solid body type "A" gave high friction and high wear. The polyimides were thus classified into three groups: Group I, low friction - high wear; Group II, high friction - low wear; and Group III, high friction - high wear.

The polyimides were classified into the three groups not only because of their friction and wear properties, but because the wear track surface morphological characteristics of each group were similar. Representative photomicrographs of each group are shown in Fig. 5.

Group I wear surfaces were characterized by being covered with powdery, agglomerated, birefringent polyimide wear particles. The wear process appeared to be adhesive, but the surface layer appeared to be brittle, and crumbling of it readily occurred. Transfer films to the pin were found to be thin and plastically flowing.

Group II polyimides were characterized by a rough-looking surface with wedge-shaped areas (Fig. 5). Wear particles were very fine and did not tend to agglomerate on the wear track. One polyimide in this group (PIC-2) produced wear surfaces that had only localized wedged-shaped areas, and the wear track for the most part was very smooth.

Initially, transfer for Group II polyimides was similar to Group I polyimides, but as sliding distance increased, thick transfer was produced which did not easily shear. Likewise friction coefficients were initially low (similar to Group I) but as transfer built up, the friction coefficient increased until a steady-state value was obtained (Fig. 6).

Group III polyimides produced very irregularly shaped wear surfaces with thick plastically flowing surface layers that tended to spall, and produced considerable back transfer (Fig. 5(c)). Transfer and friction were similar to Group II polyimides, that is, thick nonshearing transfer films built up with sliding distance, which increased friction.

Temperature and Atmosphere Effects - The elevated temperature properties of polyimide films PIC - 3, PIC - 5, and solid body types "A" and "V" have not been evaluated, but the other five have all been found to possess trans-



itions in the friction and wear properties at elevated temperatures. What is meant by a transition is that above some particular temperature both the friction coefficients and wear rates of the films drop dramatically.

When this occurs the wear surface on the polyimide film also changes. Figure 7 gives a typical example of a PIC - 1 film which was evaluated at 150° C in dry air. The wear track has become very smooth and featureless. Wear particles have been observed to spall from the surface in very thin layers, indicating that a thin-textured layer developed on the surface. Also transfer films tended to remain thin and did not build up with sliding duration.

In addition to temperature, atmosphere can have a marked effect on the tribological properties of polyimides. Figure 8 plots average friction coefficient and polyimide wear rate as a function of temperature for PIC - 1 polyimide films in three different atmospheres: Dry argon (<100 ppm H<sub>2</sub>O), dry air (<100 ppm H<sub>2</sub>O), and moist air (10 000 ppm H<sub>2</sub>O). In both dry air and dry argon, a transition in the friction and wear properties of polyimide occurred between 25° and 100° C (Fig. 8). But in moist air, the transition appears to have occurred above 100° C. A proposed cause (16 and 35) is that the H<sub>2</sub>O molecules hydrogen-bond to the polyimide chains and constrain their ability to plastically flow in thin surface layers.

#### Polyimide-Bonded Solid Lubricant Films

Wear Mechanisms - Solid lubricants are often added to polymer films to improve friction and wear properties, but they can also change the mechanisms of lubrication. MoS<sub>2</sub> and (CF<sub>x</sub>)<sub>n</sub> were added to PIC - 1 polyimide films (9). The presence of the solid lubricant reduced the strength of the polyimide and the film could not support the sliding hemisphere under a 9.8 N load. The polyimide-bonded (CF<sub>x</sub>)<sub>n</sub> film developed a series of fine cracks in

the film wear track which led to the film crumbling away in less than 15 kc of sliding (Fig. 9).

The film had been applied to a sandblasted disk. Once through the film, the polyimide and  $(CF_x)_n$  materials compacted into the valleys between the sandblasted asperities and flat plateaus were worn on the metallic asperities (Fig. 9(c)). The lubrication process then became shearing of very thin lubricant films between flats on the pin and on the asperity plateaus.

If the contact stresses applied to the polyimide-bonded  $(CF_x)_n$  films were reduced, the bonded film could support the load and wear in a manner similar to the polyimide film alone (36). An example of this is shown in Fig. 10 where a 0.95 mm - diameter flat slid against a film under a 7 MPa (1000 psi) projected contact stress (assuming full contact). The photomicrographs (Fig. 10) show the same area on the wear track after 5 and 60 kc of sliding. It is seen that the film asperities support the load and that wear is a gradual process of asperity truncation. When the film wear track is looked at under higher magnifications, the polyimide and graphite fluoride are indistinguishable and appear to have mixed together to form a very thin-textured layer (Fig. 11). The primary wear mechanism appears to be the spalling of these layers (Fig. 11).

Friction And Wear Rates - The friction and wear properties of polyimide-bonded  $(CF_x)_n$  and polyimide-bonded  $MoS_2$  films were evaluated (9) for a hemisphere sliding against the films under a 9.8 N load in dry air (<100 ppm  $H_2O$ ). Neither film supported the load, so the secondary film wear mechanism occurred. Table 3 gives friction and wear results for those experiments. Except for slightly higher friction coefficients, polyimide-bonded  $(CF_x)_n$  films gave considerably better tribological results than did polyimide-bonded  $MoS_2$  films.

As mentioned in the previous section, when contact stresses are low enough, a polyimide-bonded  $(CF_x)_n$  film itself can support the load; and wear becomes the gradual process of wearing through the film. The effect of varying the contact stress on the friction and wear of the film was investigated by applying different loads to various flat contact areas (17). Table 4 summarizes the results of those experiments, and Fig. 12 gives the wear rate results. The results indicate that both contact stress and pin contact area can affect the film wear rate.

Surface morphology studies of the wear track indicate that the above two parameters can effect the type of wear taking place. Under low stresses and small contact areas, a textured layer on the film wear track results. The wear process is the gradual spallation of this layer. Under higher contact stresses, brittle fracture of the film occurs with the size of the fractured particle depending upon the stress. Large contact areas promote the buildup of thick transfer films which increase adhesion, and thus wear, of the film.

The friction coefficient tends to be slightly higher (compared to the secondary film mechanism) when this mechanism occurs. The friction coefficient also tends to increase with sliding distance for the larger contact areas because of the buildup of thick, nonflowing transfer films. Table 4 gives the friction coefficients obtained in these experiments after various sliding intervals.

#### Polyimide Composites

Friction and Wear - To reduce the friction and wear of polymer solid bodies, solid lubricant additives are often added to them to make composites. In Ref. (23), graphite fibers were incorporated into the polyimide matrix for this purpose and to increase the load-carrying capacity. In that study,

three different GFRPI composites were evaluated using a weight ratio of 1-to-1 polyimide-to-graphite fiber constituents. Two different polyimides and two different graphite fibers were made into composite disks and slid against 440C HT stainless steel pins. Included for comparison is a commercially available type "V" polyimide composite which contained 15 percent graphite powder.

At 25° C in moist air (50 percent R.H.), the polyimide type or graphite fiber type had minimal influence on the friction coefficient obtained with these composites (Fig. 13); but when compared to one of the polyimides (PIC-7, Table 2), evaluated as a film with no additives, the friction is higher (0.20 vs 0.10). The composite made with the type "V" polyimide and 15 percent graphite powder gave higher friction than those made with graphite fibers (0.37 vs 0.20); but compared to type "V" polyimide solid bodies with no solid lubricant additives, the friction is lower, 0.37 vs 0.52 (Table 2).

Wear volume as a function of sliding distance at 25° C for the four polyimide composites is shown in Fig. 14. As found for the films and solid bodies, wear volume increased at a relatively constant rate with increasing sliding distance. Table 5 summarizes the wear rates calculated from these curves and for similar curves obtained at 300° C. At 25° C, the GFRPI composites gave up to five times less wear than did the polyimide-graphite powder composite. In fact, for this particular sliding configuration, adding graphite powder to the polyimide did not improve the wear resistance (Table 2). At 300° C, the wear rates obtained for all GFRPI composites were equivalent to or better than those obtained at 25° C. Friction coefficients at 300° C were from two to four times lower than those obtained at 25° C (Table 5).

Experiments were also conducted on the GFRPI composites in dry air

(<100 ppm H<sub>2</sub>O), since potential applications of these composites are where there is no or minimal H<sub>2</sub>O present. At 25° C, slightly lower friction coefficients and nearly equal wear rates were obtained in dry air as compared to moist air (Table 5). But at 300° C, higher friction coefficients and wear rates were obtained in dry air. One exception was that the composite made from type "A" polyimide and type "L" graphite fibers gave a slightly lower friction coefficient in dry air than in moist air at 300° C. A possible reason for this will be given in the next section.

Wear Mechanisms - Adding 15 percent graphite powder to the type "V" polyimide did not affect the wear process of the base polyimide solid. A photomicrograph of a typical wear track surface (Fig. 5) shows brittle fracture and spalling of a surface layer 1 to 2 μm thick. The graphite particles can be seen in the matrix and appear not to mix with the polyimide to form a thin surface layer as graphite fluoride did with the bonded films (Fig. 11).

For GFRPI composites formulated with type "H" fibers and evaluated in moist air, a typical wear track surface (Fig. 16) shows the general outline of the fibers which tend to flow into the polyimide at the surface. In contrast to type "H" fibers, type "L" fibers tend to completely mix together with the polyimide to form a thin surface layer less than 1 μm thick. Wear occurs by the spalling of this layer (Fig. 17).

At 300° C in moist air, neither fiber mixed with the polyimide (Fig. 18). Instead a very thin layer of the polyimide tended to flow over the fibers and dominated the lubrication process. As mentioned previously, above a transition temperature some polyimides produced very low friction and wear.

At 25° C in dry air, the surfaces were similar to those found in moist air; but at 300° C in dry air the fibers tended to crack and spall on the composite wear track (Fig. 19). The breaking up of the fibers tended to

produce higher wear rates and friction coefficients (Table 5). One exception was the type "A" polyimide with type "L" fibers. Even though wear rate increased with this composite in dry air, friction coefficient remained low at a value of 0.02. The most probable reason for this was that the polyimide for this particular composite was able to remain the dominating influence, whereas with the other composites the graphite dominated.

Configuration Effects - To compare geometry effects, the specimen configuration was reversed: a hemispherically tipped composite pin was slid against a metallic disk. The composite was made from a type "A" polyimide and from type "L" graphite fibers. With this geometry, friction increased with sliding duration (Fig. 20) in contrast to the relatively constant friction coefficient (0.2) which was obtained with the composite disk. Initially, the wear rate was lower ( $0.4 \times 10^{-14} \text{ m}^3/\text{m}$ ), but increased to  $1.2 \times 10^{-14} \text{ m}^3/\text{m}$  after 30 km of sliding, a value about the same as the composite disk ( $1.5 \times 10^{-14} \text{ m}^3/\text{m}$ ).

The increase in friction appeared to be caused by a similar phenomenon that occurred with films of polyimide and polyimide-bonded graphite fluoride. As sliding duration increased, thick, nonshearing transfer films developed, which increased friction and composite wear. Figure 21 shows transfer after 1 km of sliding when friction was relatively low ( $\mu = 0.31$ ) and after 40 km of sliding when the friction coefficient had risen to 0.58. In addition to transfer to the metallic counterface, backtransfer to the composite tended to occur when friction increased to high values. Figure 22 gives photomicrographs of the composite surface for the same sliding intervals given in Figure 21.

Friction and wear data from these experiments are compared in Table 6 to data where the GFRPI composite was used in an end-use application, a plain

spherical bearing (21). It is interesting to note that the friction and wear results from the plain spherical bearing and the pin-on-disk experiments compare very closely when the metal pin slid against the GFRPI composite disk. But, when a GFRPI composite pin slid against the metallic disk, friction and wear results were entirely different. It is believed the reasons for these differences were due to difference in wear surface morphology (caused by geometry differences) in transfer films, in projected contact stresses, and possibly to differences in temperatures in the contact areas.

#### CONCLUDING REMARKS

The tribological properties of polyimide films, polyimide solid bodies, polyimide-bonded solid lubricant films, and polyimide composites have been discussed and compared. The results indicate they have considerable promise for self-lubricating applications to temperatures of 350° C in air; however, the upper temperature limit is dependent on which type of polyimide is used and the nature of the application.

In general, the polyimides tend to be somewhat brittle and wear occurs by the brittle fracture of the surface (up to 3  $\mu\text{m}$  or more depending upon the contact stresses applied). To obtain optimum lubrication with polyimides, shear must occur in very thin surface layers (<1  $\mu\text{m}$ ). Some polyimides possess a transition temperature above which the molecules can obtain a degree of freedom necessary to plastically flow in these thin layers; but  $\text{H}_2\text{O}$  molecules from the atmosphere can hydrogen-bond to the molecular chains and constrain their motion. Thus, the transition is either masked in the presence of water vapor or translated to a higher temperature.

Thus, the problem is to alter the polyimide to induce the formation of thin surface layers at ambient temperatures in moist air. The addition of solid lubricants can help in this, but the solid lubricant must be compatible

with the polyimide in order that they mix together to form the very thin surface layers. In that regard, graphite fluoride  $((CF_x)_n)$  works well with polyimide in that the two mix together and shear in a very thin surface layer under light contact stresses.

A disadvantage of adding powdered solid lubricants (such as  $(CF_x)_n$ ) is that they tend to reduce the load-carrying capacity of the film or composite, probably due to the fact they have planes of easy shear. Graphite fibers added to polyimide solids reinforced the structure and thus improved the load-carrying capacity, but different fibers can produce different tribological results. Low modulus, graphitic fibers tended to mix with the polyimides to produce a thin shear film better than high modulus nongraphitic fibers, but low modulus fibers tended to produce thick nonshearing transfer films which tended to increase friction and wear with sliding distance.

The production of thick, nonshearing transfer films was a problem (in producing higher friction and wear) with polyimides with or without solid lubricant additives at temperatures below the transition. It is believed that this problem can be mitigated by proper additive formulation or through sliding configuration design changes, such as smaller contact areas and higher contact stress levels.

#### REFERENCES

1. Lancaster, J. K., "Dry Bearings: A Survey of Materials and Factors Affecting Their Performance," Tribology, 6 (6), 219-251 (1973).
2. Hermanck, F. J., "Coatings Lengthen Jet Engine Life," Metal Progress, 97 (3) 104-106 (1970).



3. Theberge J. "Properties of Internally Lubricated Glass - Fortified Thermoplastics for Gears and Bearings," ASLE Proceedings - International Conference on Solid Lubrication, S P 3, 166-184 (1971).
4. Brown, R. D. and Blackstone, W. R., "Evaluation of Graphite Fiber Reinforced Plastic Composites for Use in Unlubricated Sliding Bearings", Composite Materials: Testing and Design (Third Conference), ASTM STP-546, ASTM 457-476 (1974).
5. Sliney, H. E. and Johnson, R. L., "Graphite Fiber Polyimide Composites for Spherical Bearings to 340° C (650° C)," NASA T N D - 7078 (1972).
6. Bangs, S., "Foil Bearings Help Passengers Keep Their Cool," Power Transm. Des., 15 (2), 27-31 (1973).
7. Gardos, M. N. and McConnell, B. D., "Development of High-Load, High-Temperature, Self-Lubricating Composite - part I: Polymer Matrix Selection," ASLE Preprint No. 81 - LC - 3A - 3 (1981).
8. Todd, N. W., and Wolff, F. A., "Polyimide Plastics with Stand High Temperatures," Mater Des. Eng., 60 (2), 86-91 (1964).
9. Fusaro, R. L. and Sliney, H. E., "Graphite Fluoride as a Solid Lubricant in a Polyimide Binder," NASA TN D - 6714, (1972).
10. Fusaro, R. L., "Comparison of the Weight Loss and Adherence of Nine Different Polyimide Films Thermally Aged at 315° C and 350° C in Air," NASA TM - 81381, (1980).
11. Sroog, C. E., Endry, A. L., Abramo, S. V., Berr, C. E., Olivier, K. L. and Edwards, W. M., "Aromatic Polypyromellitimides from Aromatic Polyamic Acids," J. Polymer S., PT. A., 3 (4), 1373-1390 (1965).
12. Heacock, J. F., and Berr, C. E., "Polyimides - New High Temperature Polymers: H-Film, a Polypyromellitimide Film," SPE trans 5 (2), 105-110 (1965).

13. Adrova, N. A., Bessonov, M. I., Latus, I. A., and Rudakov, A. P., "Polyimides: A New Class of Thermally Stable Polymers," Progress in Materials Science Series, vol. 7 Technomic Publishing Co., Inc. (1970).
14. Fusaro, R. L., "Effect of Thermal Aging on the Tribological Properties of Polyimide Films and Polyimide Bonded Graphite Fluoride Film," Libr. Eng., 36 (3), 143-153 (1980).
15. Fusaro, R. L., "Tribological Properties at 25° C of Seven Polyimide Films Bonded to 440° C High-Temperature Stainless Steel," NASA TP-1944, 1982.
16. Fusaro, R. L. "Effect of Atmosphere and Temperature on Wear, Friction, and Transfer of Polyimide Films," ASLE trans., 21 (2) 125-133 (1978).
17. Fusaro, R. L., "Effect of Load Area of Contact and Contact Stress on the Wear Mechanisms of a Bonded Solid Lubricant Film," Wear, 75 403-422 (1982).
18. Giltrow, J. P. and Lancaster, J. K., "Properties of Carbon-Fibre-Reinforced Polymers Relevant to Applications in Tribology," London, Plastics Institute, International Conference on Carbon Fibres, Their Composites and Applications, Paper 31, (Feb. 1971).
19. Giltrow, J. P. and Lancaster, J. D., "Friction and Wear of Polymers Reinforced with Carbon Fibers," Nature, 214, 1106-1107 (1967).
20. Lancaster, J. K., "The Effect of Carbon Fibre Reinforcement on the Friction and Wear of Polymers," J. Phys. D., 1, 549-559 (1968).

21. Sliney, H. E. and Jacobson, T. P., "Performance of Graphite Fiber-Reinforced Polyimide Composites in Self-Aligning Plain Bearings to 315° C," Lubr. Eng. 31 (12), 609-613 (1975).
22. Sliney, H. E. and Jacobson, T. P., "Some Effects of Composition on Friction and Wear of Graphite-Fiber-Reinforced Polyimide Liners in Plain Spherical Bearings," NASA TP-1229, (1978).
23. Fusaro, R. L. and Sliney, H. E., "Friction and Wear Behavior of Graphite Fiber Reinforced Polyimide Composites," ASLE Trans., 21 (4), 337-343 (1978).
24. Lancaster, J. K., "Geometrical Effects on the Wear of Polymers and Carbons," J. Lubr. Technol., 97 (2), 187-194 (1975).
25. Sliney, H. E., "Some Load Limits and Self-Lubricating Properties of Plain Spherical Bearings with Molded Graphite Fiber-Reinforced Polyimide Liners to 320° C," Lubr. Eng., 35 (9), 497-502 (1979).
26. Fusaro, R. L., "Geometrical Aspects of the Tribological Properties of Graphite Fiber Reinforced Polyimide Composites," ASLE Preprint No. 82 - AM - SA - 2 (1982).
27. Gardos, M. N. and McConnell, B. D., "Development of a High-Load High-Temperature, Self-Lubricating Composite - Part II: Reinforcement Section, Part III: Additives Section, Part IV: Formulation and Performance of the Best Compositions," ASLE Preprint No. 81 - LC - 3A - 4, 81 - LC - 3A - 5, and 81 - LC - 3A - 6 (1981).
28. Giltrow, J. P., "A Design Philosophy for Carbon Fibre Reinforced Sliding Components," Tribology, 4 (1) 21-28 (1971).
29. Harris, C. L. and Wyn-Roberts, D., "Wear of Carbon-Fibre Reinforced Polymers in High Vacuum Environment," Nature, 217, 981-982 (1968).

30. Giltrow, J. P. and Lancaster, J. K., "Carbon-Fibre Reinforced Polymers as Self-Lubricating Materials. Tribology Convention, Pitlochry, Scotland, May 15-17, 1968, Proceedings, Institution of Mechanical Engineers, 149-159 (1968).
31. Giltrow, J. P. and Lancaster, J. K., "The Role of the Counterface in the Friction and Wear of Carbon Fibre Reinforced Thermosetting Resins," Wear, 16 (11), 359-374 (1970).
32. Simon, R. A. and Prosen, S. P., "Graphite Fiber Composites; Shear Strength and Other Properties," Twenty-Third Annual Technical Conference, SPI Reinforced Plastics Composite Division, Proceedings, Society of the Plastics Industry, Inc., Section 16-B, 1-10 (1968).
33. Herrick, J. W., "Bearing Materials from Graphite Fiber Composites," Reinforced Plastics - Ever New; Proceedings of the Twenty-Eighth Annual Technical Conference, Society of the Plastics Industry, Inc., 17-D, 1-17-D, 6, (1973).
34. Giltrow, J. P., "The Influence of Temperature on the Wear of Carbon Fiber Reinforced Resins," ASLE Trans., 16 (2), 83-90 (1973).
35. Fusaro, R. L., "Molecular Relaxations, Molecular Orientation, and Friction Characteristics of Polyimide Films," ASLE Trans., 20 (1), 1-14 (1977).
36. Fusaro, R. L., "Lubrication and Wear Mechanisms of Polyimide-bonded Graphite Fluoride Films Subjected to Low Contact Stress," NASA TP-1584, (1980).

Table 1 - Typical Graphite Fiber Properties

Property or Characteristic	TYPE "L"		TYPE "H"	
	English Units	SI Units	English Units	SI Units
Tensile strength	$9.0 \times 10^4$ lb/in <sup>2</sup>	$6.2 \times 10^8$ N/m <sup>2</sup>	$2.8 \times 10^5$ lb/in <sup>2</sup>	$2.0 \times 10^9$ N/m <sup>2</sup>
Elastic modulus	$5.0 \times 10^6$ lb/in <sup>2</sup>	$3 \times 10^{10}$ N/m <sup>2</sup>	$5.7 \times 10^7$ lb/in <sup>2</sup>	$3.9 \times 10^{11}$ N/m <sup>2</sup>
Length	0.25 in	$6.4 \times 10^{-3}$ m	0.25 in	$6.4 \times 10^{-3}$ m
Diameter	$3.3 \times 10^{-4}$ in	$8.4 \times 10^{-6}$ m	$2.6 \times 10^{-4}$ in	$6.6 \times 10^{-6}$ m
Specific Gravity	1.4	1.4	1.8	1.8

Table 2 - Classification of Polyimides into Three Friction and Wear Groups for Ambient Temperature Conditions (22° to 27° C in 50 percent RH air).

(Disk material, polyimide film or solid body; rider material, hemispherically-tipped 440C HT stainless steel rider; load, 9.8 N; sliding speed, 2.7 m/s (1000 rpm)).

Polyimide Designation	Film or Solid	Average "Steady-State" Friction Coefficient	Average Film Wear Rate, m <sup>3</sup> /m	Group Characteristics	Group Number
PIC - 1	Film	0.13	$40 \times 10^{-14}$	Low Friction- High Wear	I
PIC - 4	Film	.13	$80 \times 10^{-14}$		
PIC - 7	Film	.10	$40 \times 10^{-14}$		
PIC - 2	Film	.23	$10 \times 10^{-14}$	High Friction- Low Wear	II
PIC - 3	Film	.27	$6 \times 10^{-14}$		
PIC - 5	Film	.30	$6 \times 10^{-14}$		
PIC - 6	Film	.28	$12 \times 10^{-14}$		
"V"	Solid	.52	$10 \times 10^{-14}$	High Friction- High Wear	III
"A"	Solid	.42	$35 \times 10^{-14}$		

Table 3 - Friction and Wear Results for a Hemispherically Tipped Pin  
 Sliding on Polyimide Bonded MoS<sub>2</sub> or (CF<sub>x</sub>)<sub>n</sub> Films  
 During the Secondary Film Lubricating Mechanism

(Disk substrate, sandblasted 440C HT stainless steel; pin material, 440C HT stainless steel; load, 9.8N; sliding speed, 2.7 m/s (1000 rpm); atmosphere, dry air (<10000m H<sub>2</sub>O)).

Temperature, °C	Low Average Friction Coefficient		Endurance * life kc		Rider Wear Rate		10 <sup>-15</sup> m <sup>3</sup> /m	
	MoS <sub>2</sub>	(CF <sub>x</sub> ) <sub>n</sub>	MoS <sub>2</sub>	(CF <sub>x</sub> ) <sub>n</sub>	0 to 60 kc		0 to Endurance Life	
	MoS <sub>2</sub>	(CF <sub>x</sub> ) <sub>n</sub>	MoS <sub>2</sub>	(CF <sub>x</sub> ) <sub>n</sub>	MoS <sub>2</sub>	(CF <sub>x</sub> ) <sub>n</sub>	MoS <sub>2</sub>	(CF <sub>x</sub> ) <sub>n</sub>
25	.02	.08	1400	3000	.02	.005	.2	.08
100	.02	.04	560	2700	.02	.005	.2	.07
200	.02	.03	100	1800	.02	.009	.7	.7
300	.02	.03	30	480	---	.04	1.3	1.1
350	.05	---	10	---	---	---	1.9	---
400	.06	.03	4	230	---	---	3.2	4.2
500	---	.04	-	20	---	---	---	21

\* Kilocycles of sliding to reach  $\mu$  of 0.30.

Table 4 - Friction and Wear Data Obtained on PI-Bonded (CF<sub>x</sub>)<sub>n</sub> Films Under Low Projected Contact Stresses

Load Rider Contact Area cm <sup>2</sup> (N)	Projected Rider Contact Stress MPa (lbf in <sup>-2</sup> )	Average Value of Friction Coefficient at				Test Duration, kc	Thickness of Film Worn Through, μm	Film Wear Rate, μm <sup>3</sup> in <sup>-1</sup>	
		5 kc	60 kc	500 kc	End of Test				
2.5	0.0035	7 (1000)	0.12	0.15	0.15	0.16	1190	13	0.8x10 <sup>-14</sup>
4.9	.0035	14 (2000)	.12	.14	.18	.19	565	15	2.3x10 <sup>-14</sup>
	.0071	7 (1000)	.14	.17	.19	.22	6915	15	0.29x10 <sup>-14</sup>
	.0145	3.5 (500)	.16	.19	.15	.34	7930	13	.25x10 <sup>-14</sup>
9.8	.0240	2.0 (300)	.15	.19	.19	.20	10300	8	.14x10 <sup>-14</sup>
	.0035	28 (4000)	.14	.16	-	.16	400	15	2.9x10 <sup>-14</sup>
	.0071	14 (2000)	.13	.19	.22	.28	3500	39	1.7x10 <sup>-14</sup>
14.7	.0145	7 (1000)	.16	.20	.23	.23	11670	30	0.60x10 <sup>-14</sup>
	.0240	4.1 (600)	.16	.21	.34	.29	4340	10	.27x10 <sup>-14</sup>
	.0035	42 (6000)	.13	.22	.22	.22	500	14	5.5x10 <sup>-14</sup>
19.6	.0071	21 (3000)	.13	.19	.16	.20	690	14	2.6x10 <sup>-14</sup>
	.0035	56 (8000)	.13	.13	-	.13	65	23	46.0x10 <sup>-14</sup>
	.0071	28 (4000)	.14	.15	.17	.18	800	21	4.9x10 <sup>-14</sup>
29.4	.0145	14 (2000)	.16	.24	.28	.26	1110	16	2.4x10 <sup>-14</sup>
	.0240	8.1 (1200)	.16	.20	.19	.31	2200	25	2.2x10 <sup>-14</sup>
	.0071	42 (6000)	.13	.13	-	.13	45	21	55.0x10 <sup>-14</sup>
34.4	.0145	21 (3000)	.16	.26	-	.22	112	10	12.0x10 <sup>-14</sup>
	.0240	12 (1800)	.17	.24	.28	.25	910	27	6.1x10 <sup>-14</sup>
	.0145	28 (4000)	.14	.18	-	.16	90	14	34.0x10 <sup>-14</sup>
39.2	.0240	16 (2300)	.16	.19	-	.18	220	25	24.0x10 <sup>-14</sup>
	.0145	24 (3500)	.16	-	-	.18	20	14	124.0x10 <sup>-14</sup>
	.0240	24 (3500)	.16	-	-	.18	20	14	124.0x10 <sup>-14</sup>

Table 5 - Comparison of Friction Coefficients and Wear Rates of Polyimide

Composite Materials

(Disk, composite material; rider, hemispherically tipped 440C HT stainless steel pin; sliding speed, 2.7 m/s (1000 rpm); load, 9.8 N)

Type of Composite	Temperature C	Average Friction Coefficient		Average Wear Rate	
		Dry* Air	Moist** Air	Dry Air, m <sup>3</sup> /m	Moist Air, m <sup>3</sup> /m
Type "V" Polyimide	25	---	0.37	---	10x10 <sup>-14</sup>
15% graphite Powder	300	---	---	---	---
Type "A" Polyimide	25	0.09	0.20	2x10 <sup>-14</sup>	1.5x10 <sup>-14</sup>
50% Type "L" Graphite Fibers	300	0.02	0.05	6x10 <sup>-14</sup>	2x10 <sup>-14</sup>
Type "C" Polyimide	25	0.16	0.19	1x10 <sup>-14</sup>	2.5x10 <sup>-14</sup>
50% Type "L" Graphite Fibers	300	0.18	0.04	7x10 <sup>-14</sup>	2x10 <sup>-14</sup>
Type "C" Polyimide	25	0.12	0.18	3x10 <sup>-14</sup>	5x10 <sup>-14</sup>
50% Type "H" Graphite Fibers	300	0.26	0.09	8x10 <sup>-14</sup>	2x10 <sup>-14</sup>

\* 100 ppm H<sub>2</sub>O

\*\* 10 000 ppm H<sub>2</sub>O (50 percent R.H.).



Table 6 - Comparison of Friction and Wear Data Obtained on GFRPI Composites Using Different Experimental Apparatus and Geometries.

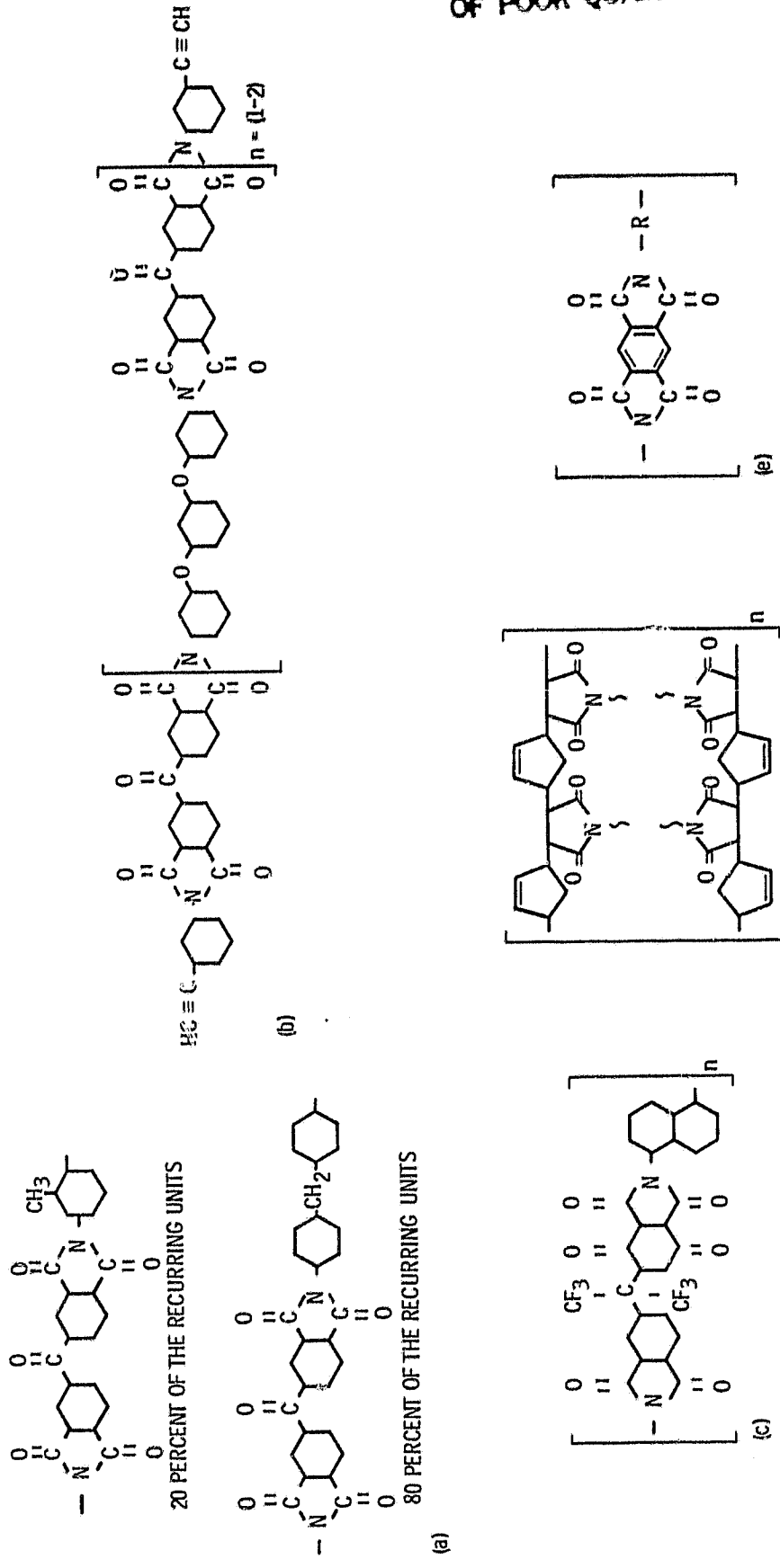
Experimental Apparatus	Composite Wear Specimen	Temperature, °C	Average Friction Coefficient	Specific Wear Rate, m <sup>3</sup> /N-m
Self-aligning plain bearings	Molded <sup>a</sup> liner	25	0.15	1.2±0.4x10 <sup>-15</sup>
		315	.05	1.2±0.4x10 <sup>-15</sup>
	Insert <sup>a</sup> liner	25	.15	2.0±1.0x10 <sup>-15</sup>
		315	.05	2.0±1.0x10 <sup>-15</sup>
Pin-on-disk	Pin <sup>b</sup>	25	.39	0.4±0.1x10 <sup>-15</sup>
		300	.50	20.0±10x10 <sup>-15</sup>
	Disk <sup>c</sup>	25	.19	1.3±0.4x10 <sup>-15</sup>
		300	.05	1.5±0.3x10 <sup>-15</sup>

<sup>a</sup>Data from Ref. 21.

<sup>b</sup>Data from Ref. 23.

<sup>c</sup>Data from Ref. 26.

ORIGINAL PAGE IS  
OF POOR QUALITY



(a) PIC-5 polyimide film. (b) PIC-6 polyimide film.  
(c) PIC-7 polyimide film, and Type "C" polyimide solid body.  
(d) Type "A" polyimide solid body. (e) Type "V" polyimide solid body.

Figure 1. - Structure and designation of polyimides used as films or as solid body composites.

ORIGINAL PAGE IS  
OF POOR QUALITY.

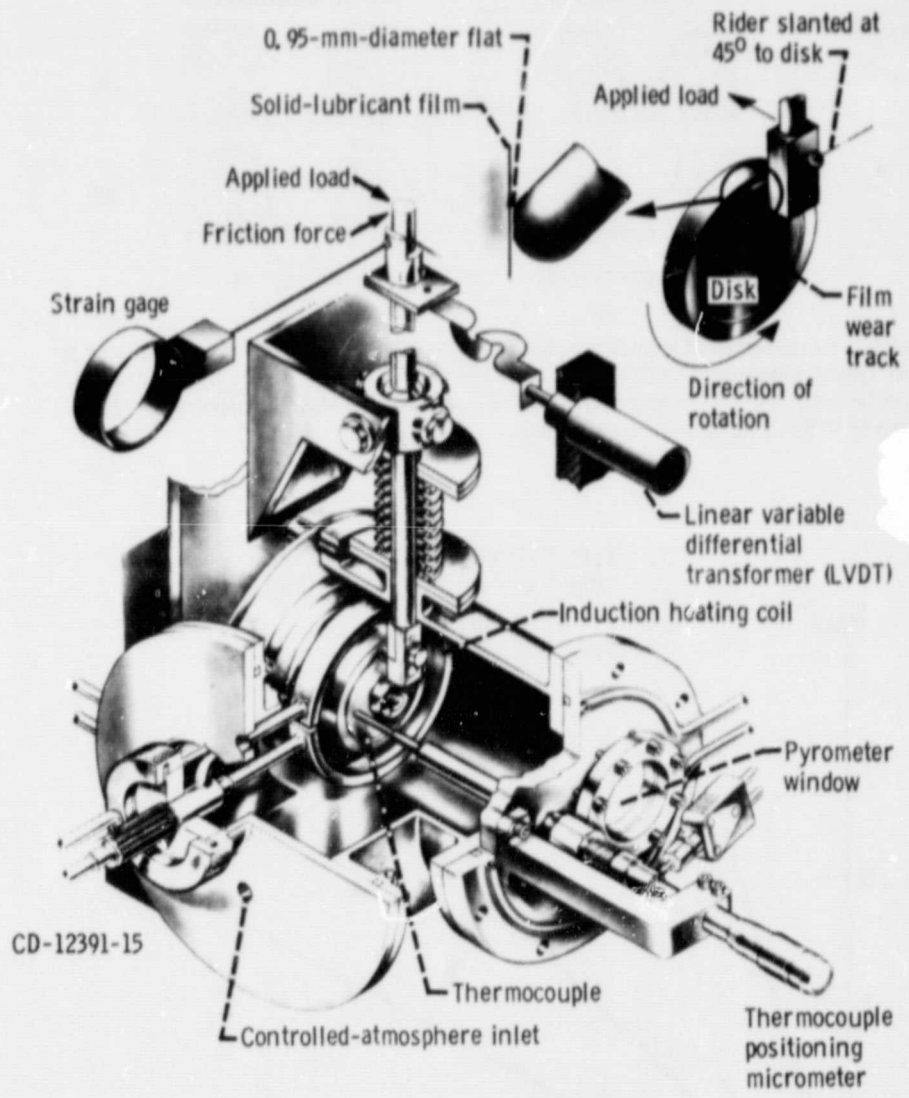


Figure 2. - Friction and wear apparatus.

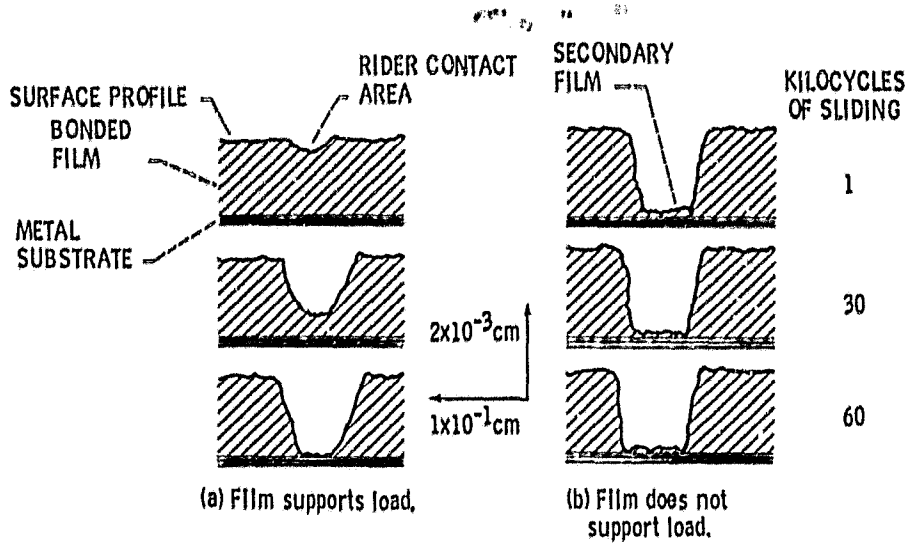


Figure 3. - Cross sectional area schematics of the wear areas on a bonded film (polymer or other type of solid lubricant film) after 1, 30 and 60 kilocycles of sliding illustrating the two different types of macroscopic lubricating mechanisms. (Note that vertical magnification is 50 times horizontal magnification.)

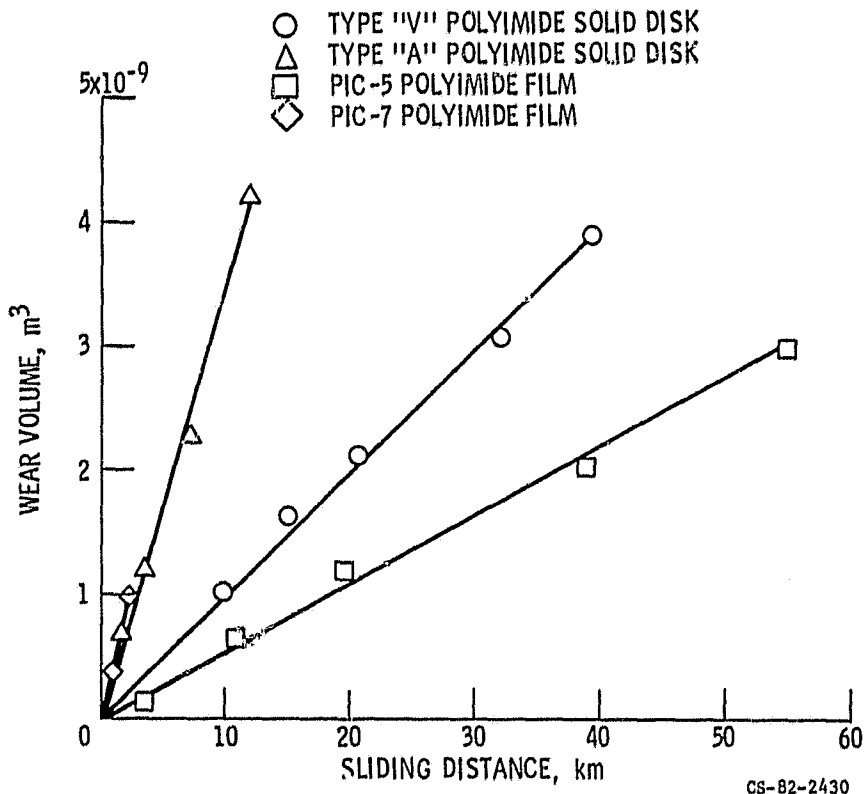
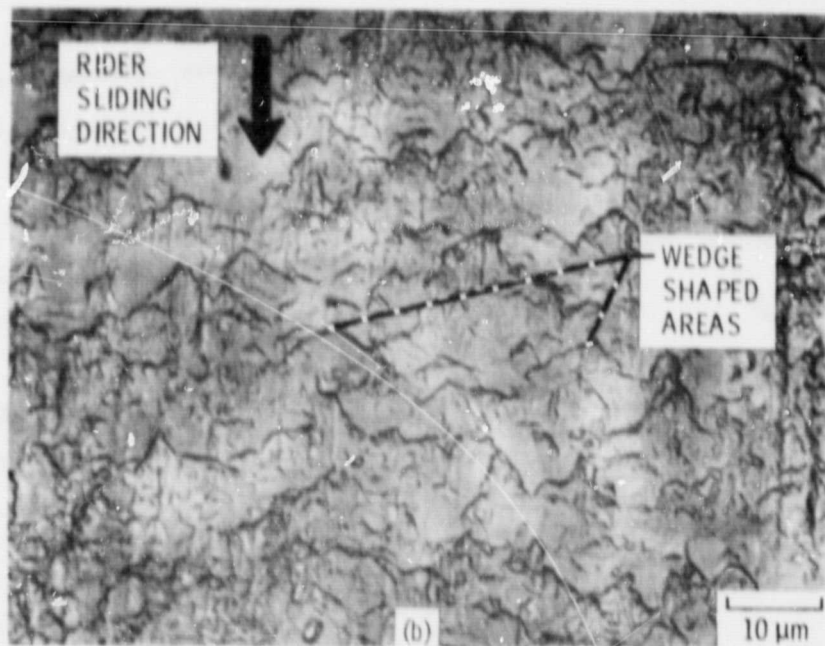


Figure 4. - Wear volume as a function of sliding distance for various polyimide film or solid body materials. (Sliding speed, 2.7 m/s; load, 9.8 N; 50% R. H. air atmosphere; 0.476cm-radius hemispherically tipped pin riders).



(a) Wear surface on Group I type of polyimide.

(b) Wear surface on Group II type of polyimide.

Figure 5. - High magnification photomicrographs illustrating the difference wear track surface morphology between Group I polyimides, Group II polyimides, and Group III polyimides.

ORIGINAL PAGE  
BLACK AND WHITE PHOTOGRAPH



(c) Wear surface on group 111 type polyimide.  
Figure 5. - Concluded.

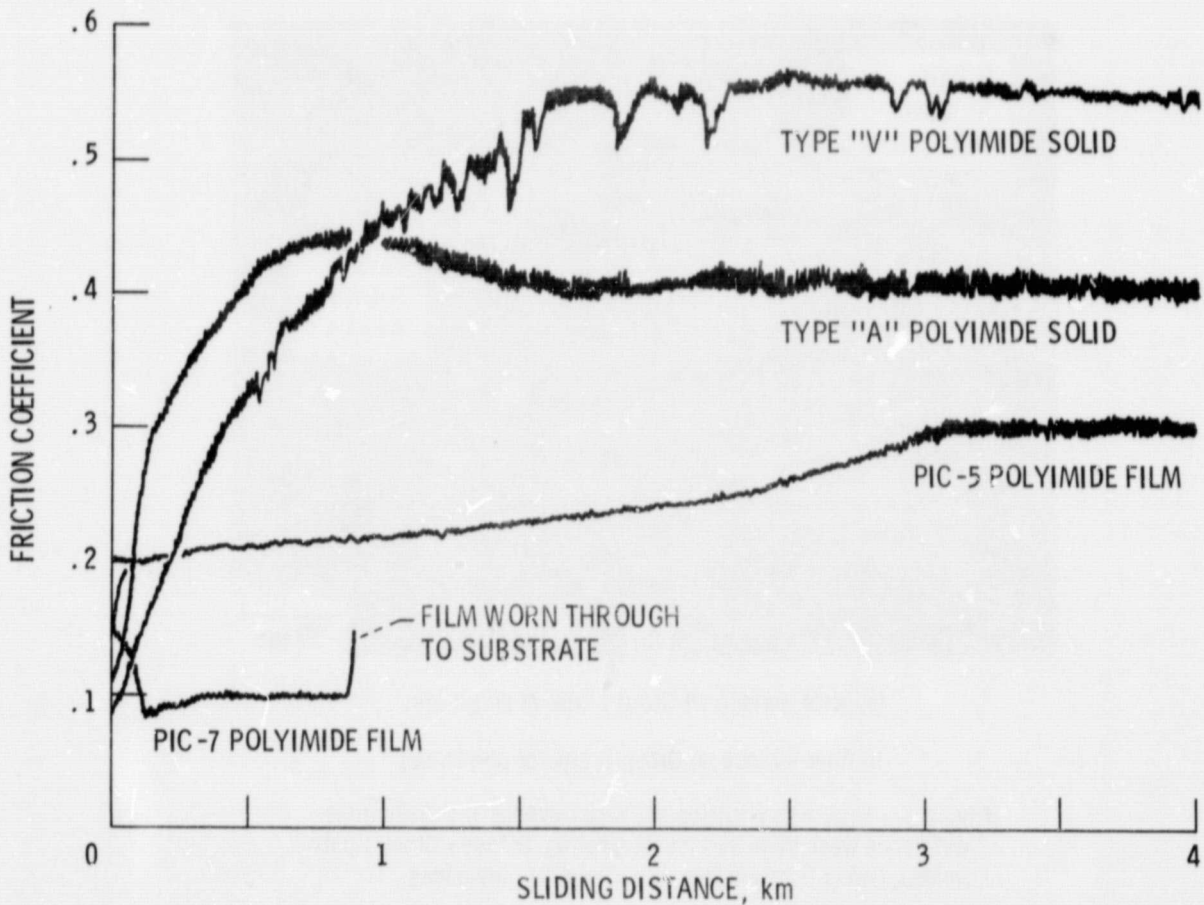


Figure 6. - Friction coefficient as a function of sliding distance (for the initial stages of sliding) for two different polyimides made into solid disks and for two different polyimides applied as films to metallic disks. (Sliding speed, 2.7 m/s; load, 9.8 N; 50% R. H. air atmosphere; 0.476 cm-radius hemispherically tipped metallic riders).

ORIGINAL PAGE  
BLACK AND WHITE PHOTOGRAPH

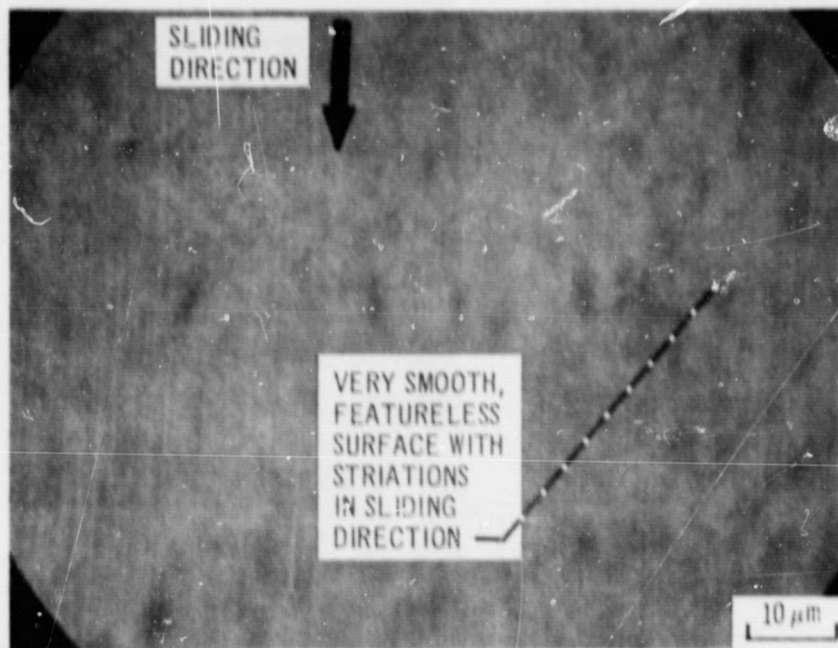
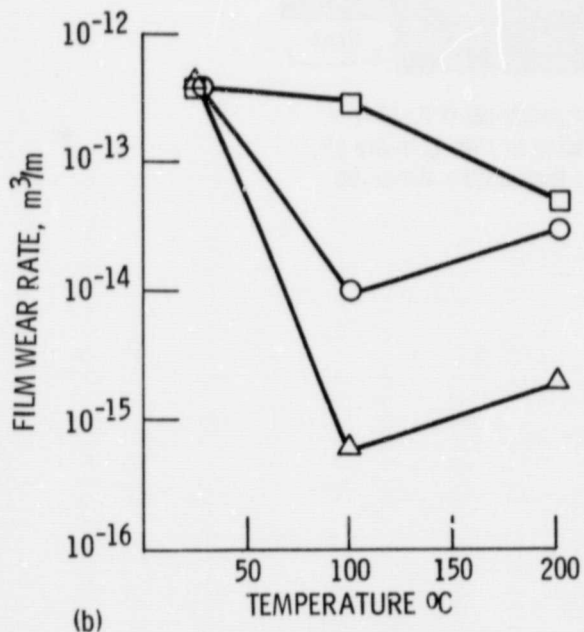
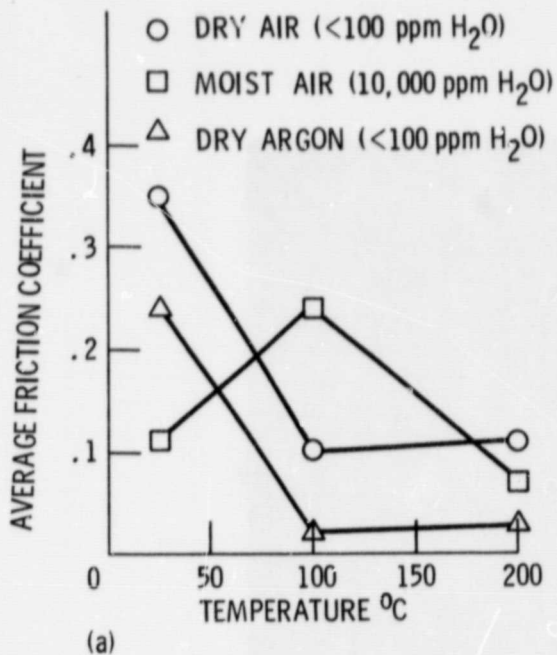
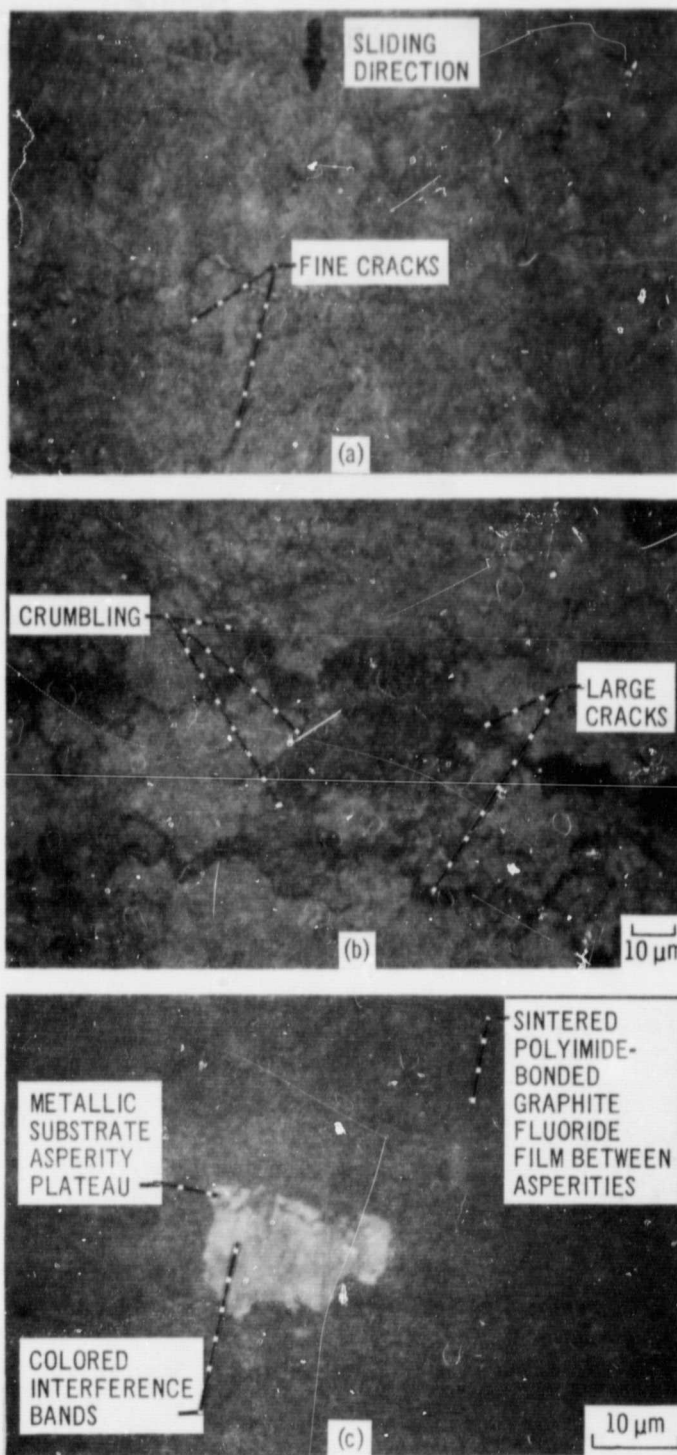


Figure 7. - High magnification photomicrograph of polyimide (PIC-1) film wear track surface after 120 kc (2 hours) of sliding at 150° C in dry air, illustrating the sliding surface morphology at a temperature above the transition.



(a) Friction coefficient.  
(b) Film wear rate.

Figure 8. - Effect of temperature and atmosphere on the friction coefficient and wear rate of polyimide films. (Specific type of polyimide film PIC-1)

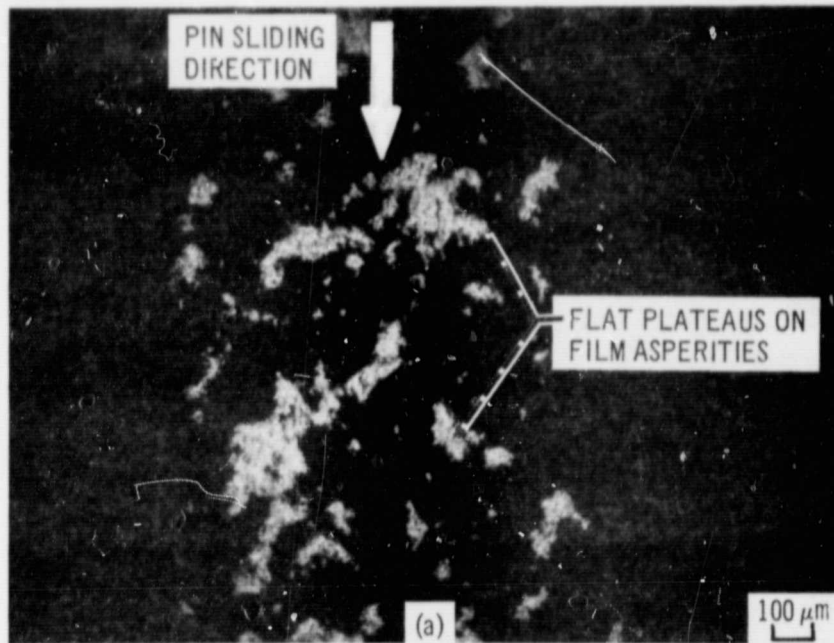


(a) 1/4 kc of sliding.  
(b) 5 kc of sliding.  
(c) 15 kc of sliding

Figure 9. - High magnification photomicrographs of the central area of the wear track (for the hemisphere sliding on a 45-micrometer-thick polyimide-bonded graphite fluoride film) after sliding intervals of 1/4, 5, and 15 kilocycles under a 9.8 N load at 1000 rpm (2.6 m/s).



ORIGINAL PAGE  
BLACK AND WHITE PHOTOGRAPH



(a) 5 kc of sliding.

(b) 60 kc of sliding.

Figure 10. - Photomicrographs of the same area on the wear track of a polyimide-bonded graphite fluoride film after sliding durations of 5 and 60 kilocycles. (Pin, 440C HT stainless steel with a 0.95 mm-diameter flat; load, 1 kg; projected contact stress, 7 MPa (1000 psi); sliding speed, 2.7 m/s (1000 rpm); 50% RH air atmosphere).

ORIGINAL PAGE  
BLACK AND WHITE PHOTOGRAPH



Figure 11. - High magnification photomicrograph of the wear track which was taken after the 0.95 mm diameter flat had slid for 1500 kc on the polyimide-bonded graphite fluoride film, showing blistering and spalling of a thin layer of the film.

ORIGINAL PAGE IS  
OF POOR QUALITY

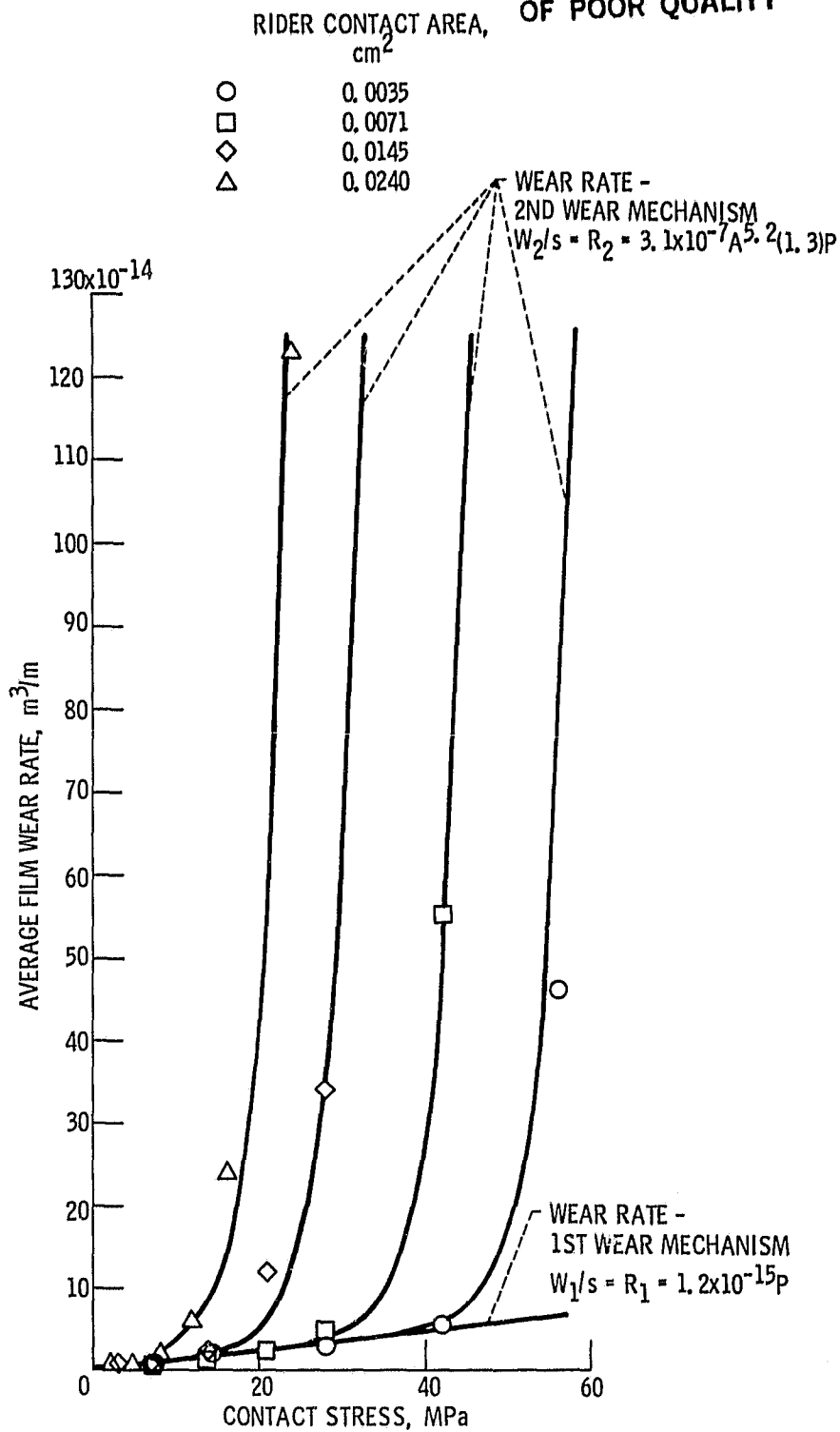


Figure 12. - Average PI-bonded ( $CF_x$ )<sub>n</sub> film wear rate experimental values as a function of contact stress showing wear rate curves which were derived from the data points. ( $R_1$  and  $R_2$  are wear rates;  $W_1$  and  $W_2$  are wear volumes;  $S$  is sliding distance,  $P$  is contact stress in MPa, and  $A$  is in flat contact area).

ORIGINAL PAGE IS  
OF POOR QUALITY

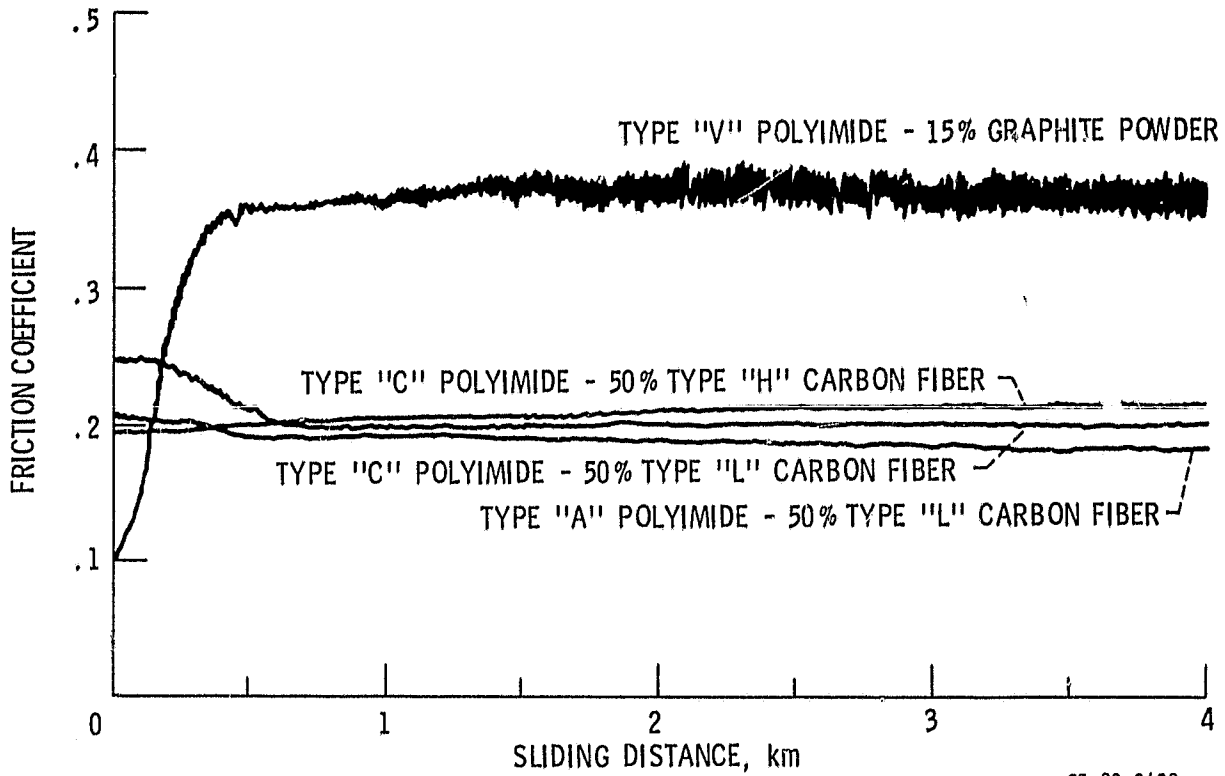


Figure 13. - Friction coefficient as a function of sliding distance (for initial stages of sliding) for polyimide composite materials made into composite disks. (Sliding speed, 2.7 m/s; load, 9.8 N; 50% R. H. air atmosphere; 0.476 cm-radius hemispherically tipped pin riders).

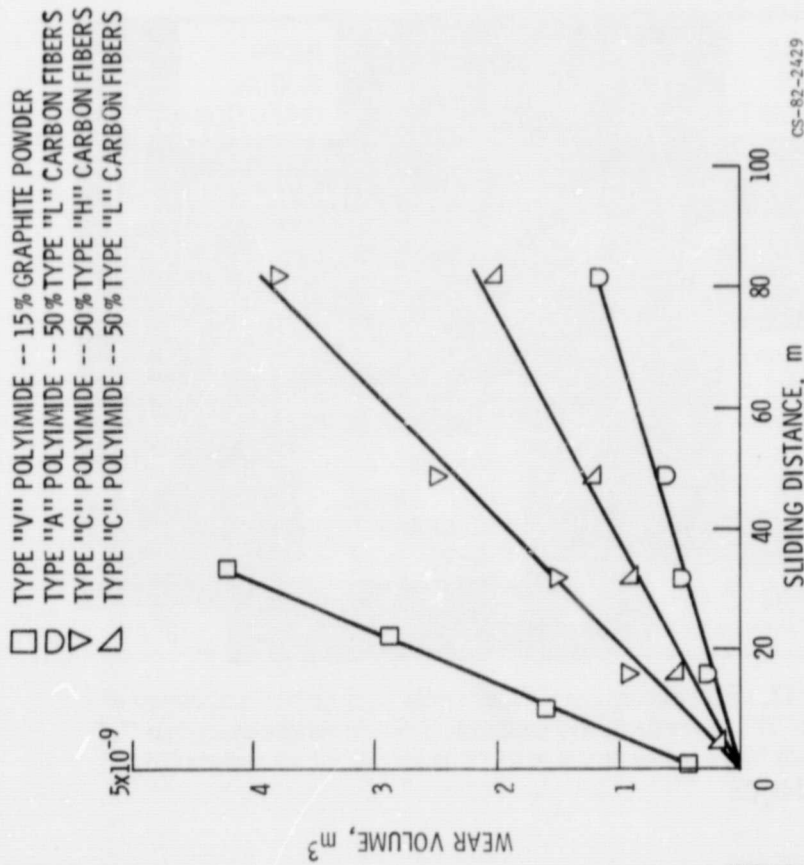


Figure 14. - Polyimide composite wear volume as a function of sliding distance for a hemispherically tipped 440C HT stainless steel pin sliding against the composite. (Temperature, 250 C; atmosphere, 50% RH air; load, 9.8 N; sliding speed, 2.7 m/s).

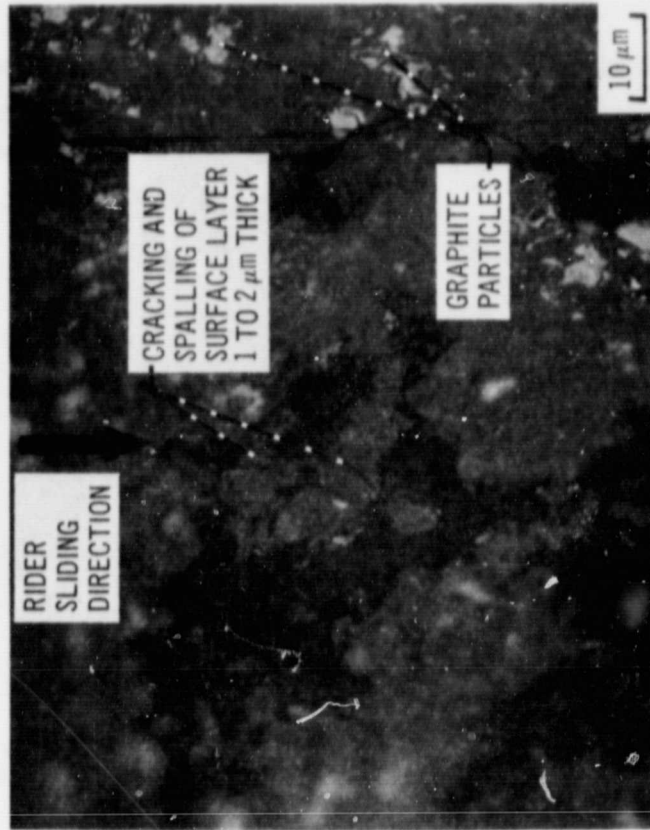


Figure 15. - Photomicrograph of typical wear surface morphology at 25° C on the type "V" polyimide composite with 15% addition of graphite powder.

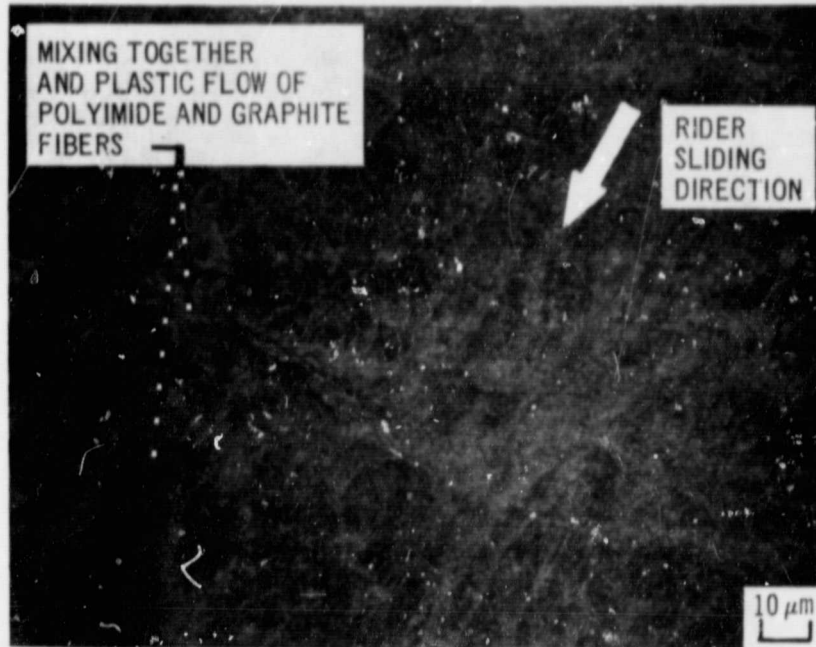


Figure 16. - Photomicrograph of typical wear track surface morphology of GFRPI composite disks formulated using type "H" carbon fibers and evaluated at 25° C in a moist air atmosphere (10,000 ppm H<sub>2</sub>O).

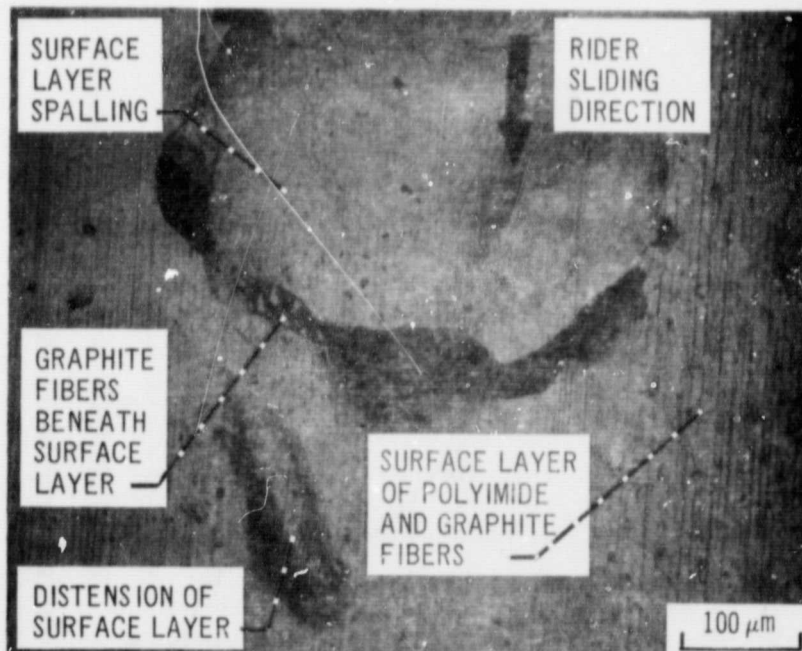


Figure 17. - Photomicrograph of typical wear track surface morphology of type "A" polyimide GFRPI composite disks formulated using type "L" carbon fibers and evaluated at 25° C in a moist air atmosphere (10,000 PPM H<sub>2</sub>O).

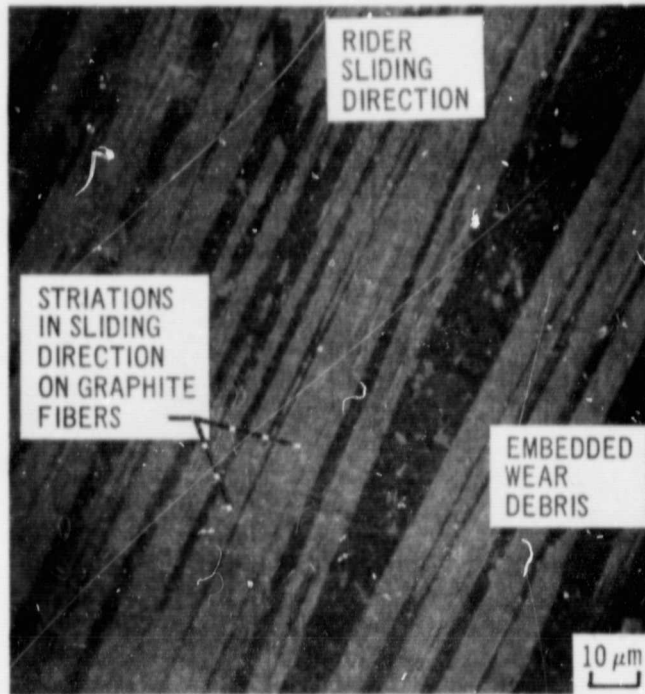


Figure 18. - Photomicrographs of the wear track surface morphology at 300° C in moist air of GFRPI composites formulated from type "A" polyimide and type "H" fibers. Similar surface morphology resulted with the other polyimide and graphite fiber under these conditions.

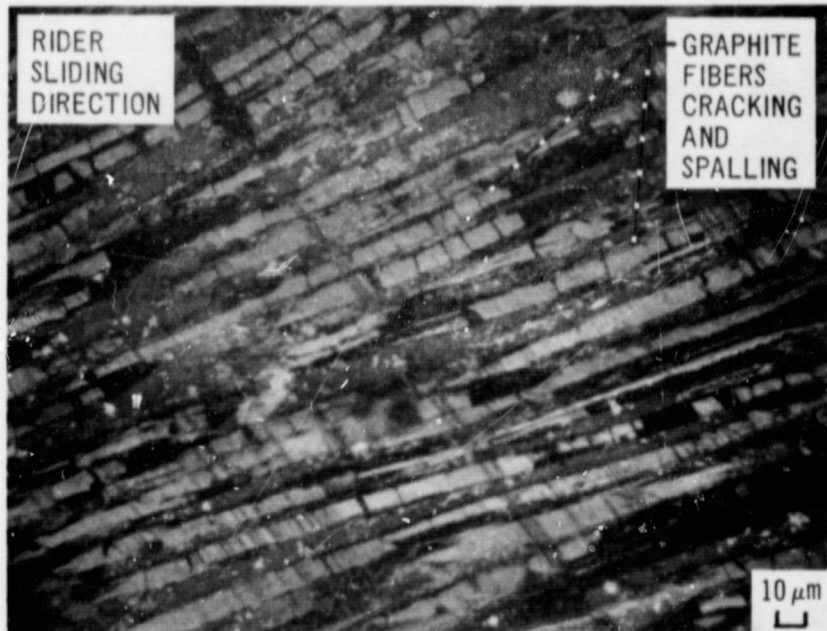


Figure 19. - Photomicrograph of typical wear track surface morphology of all GFRPI composite disks evaluated at 300° C in a dry air atmosphere (< 100 ppm H<sub>2</sub>O).

ORIGINAL PAGE  
BLACK AND WHITE PHOTOGRAPH

ORIGINAL PAGE IS  
OF POOR QUALITY

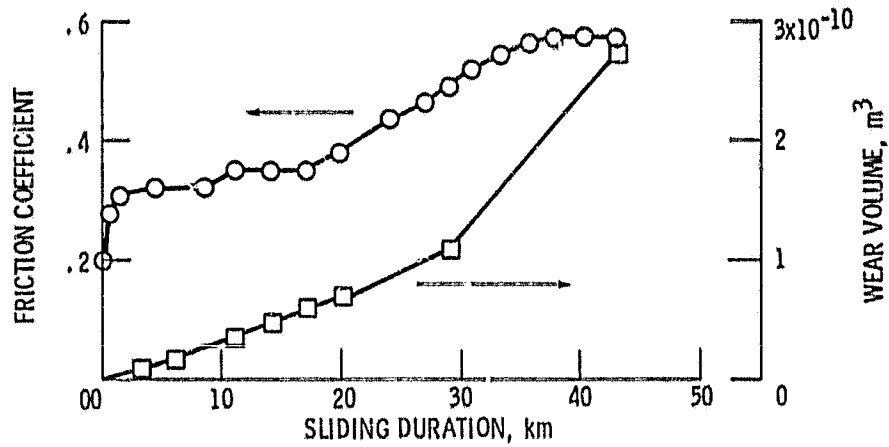
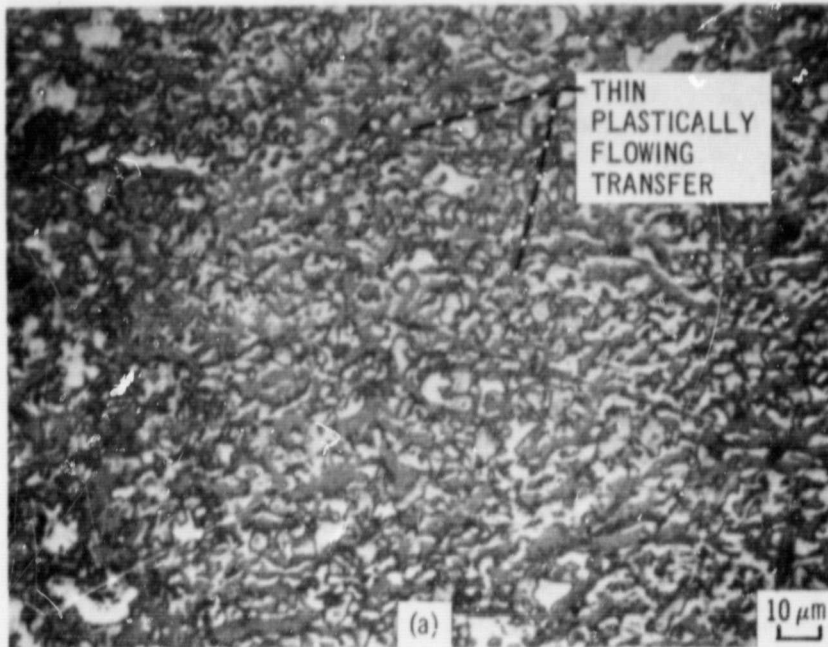


Figure 20. - Friction coefficient and GFRPI rider wear volume as a function of sliding duration. (Disk, 440C HT stainless steel; temperature, 25<sup>o</sup> C; sliding speed, 2.7 m/s; load, 9.8 N; 50% R. H. air atmosphere).



ORIGINAL PAGE  
BLACK AND WHITE PHOTOGRAPH

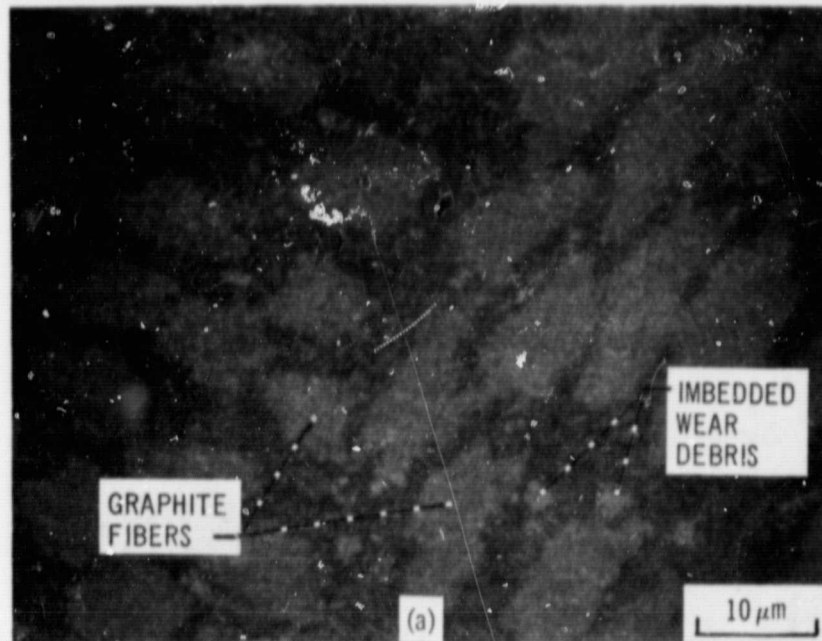


(a) 1 km of sliding,  $\mu = 0.31$ .

(b) 40 km of sliding,  $\mu = 0.58$ .

Figure 21. - Transfer to 440C HT stainless steel counterfaces from GFRPI riders (type "A" polyimide, type "L" graphite fiber) when lower friction coefficients and when higher friction coefficients were obtained. (Temperature, 25% C; atmosphere, 50% RH air; load, 9.8 N; sliding speed, 2.7 m/s.)

ORIGINAL PAGE  
BLACK AND WHITE PHOTOGRAPH



(a) 1 km of sliding,  $\mu = 0.31$ .

(b) 40 km of sliding,  $\mu = 0.58$ .

Figure 22. - Wear surface morphology of GFRPI riders (type "A" polyimide, type "L" graphite fiber) which slid on 440C HT stainless steel counter-faces when lower friction coefficients and when higher friction coefficients were obtained. (Temperature, 25° C; atmosphere, 50% RH air; load, 9.8 N; sliding speed, 2.7 m/s.)